

Proceedings of the

Advanced Architectures in Photonics

September 21–24, 2014

Prague, Czech Republic

Volume 1

Editors

Jiri Orava

University of Cambridge
Department of Materials Science and Metallurgy
27 Charles Babbage Road
CB3 0FS Cambridge
United Kingdom

Tohoku University
WPI-Advanced Institute for Materials Research
(WPI-AIMR)
2-1-1 Katahira, Aoba-ku
980-8577 Sendai
Japan

Tomas Kohoutek

Involved Ltd.
Siroka 1
537 01 Chrudim
Czech Republic

Proceeding of the Advanced Architectures in Photonics
<http://aap-conference.com/aap-proceedings>

ISSN: 2336-6036
September 2014

Published by **Involved Ltd.**
Address: Siroka 1, 53701, Chrudim, Czech Republic
Email: info@involved.cz, Tel. +420 732 974 096



This work is licensed under a
[Creative Commons Attribution
3.0 Unported License](https://creativecommons.org/licenses/by/3.0/).

CONTENTS

[Preface](#)

T. Wagner (Chairman)	i
----------------------------	---

FULL PAPERS

[Innovative nanoimprint lithography](#)

S. Matsui, H. Hiroshima, Y. Hirai and M. Nakagawa	1
---	---

[Nanofabrication by imprint lithography and its application to photonic devices](#)

Y. Sugimoto, B. Choi, M. Iwanaga, N. Ikeda, H. T. Miyazaki and K. Sakoda	5
--	---

[Soft-mould imprinting of chalcogenide glasses](#)

T. Kohoutek, J. Orava and H. Fudouzi	9
--	---

[Electric nanoimprint to oxide glass containing alkali metal ions](#)

T. Misawa, N. Ikutame, H. Kaiju and J. Nishii	11
---	----

[Producing coloured materials with amorphous arrays of black and white colloidal particles](#)

Y. Takeoka, S. Yoshioka, A. Takano, S. Arai, N. Khanin, H. Nishihara, M. Teshima, Y. Ohtsuka and T. Seki	13
--	----

[Stimuli-responsive colloidal crystal films](#)

C. G. Schafer, S. Heidt, D. Scheid and M. Gallei	15
--	----

[Opal photonic crystal films as smart materials for sensing applications](#)

H. Fudouzi and T. Sawada	19
--------------------------------	----

[Introduction of new laboratory device 4SPIN® for nanotechnologies](#)

M. Pokorny, J. Rebíček, J. Klémes and V. Velebný	20
--	----

[Controlling the morphology of ZnO nanostructures grown by Au-catalyzed chemical vapor deposition and chemical bath deposition methods](#)

K. Govatsi and S. N. Yannopoulos	22
--	----

[Visible photon up-conversion in glassy \$\(\text{Ge}_{25}\text{Ga}_{5}\text{Sb}_{5}\text{S}_{65}\)_{100-x}\text{Er}_x\$ chalcogenides](#)

L. Strizik, J. Zhang, T. Wagner, J. Oswald, C. Liu and J. Heo	27
---	----

POSTERS presented at AAP 2014

[Solution processing of As-S chalcogenide glasses](#)

T. Kohoutek	31
-------------------	----

[Ga-Ge-Sb-S:Er³⁺ amorphous chalcogenides: Photoluminescence and photon up-conversion](#)

L. Strizik, J. Oswald, T. Wagner, J. Zhang, B. M. Walsh and J. Heo	32
--	----

[Multi-wavelength and multi-intensity illumination of the GeSbS virgin film](#)

P. Knotek, M. Kincl and L. Tichý	33
--	----

[Towards functional advanced materials based using filling or ordered anodic oxides supports and templates](#)

J. M. Macak, T. Kohoutek, J. Kolar and T. Wagner	34
--	----

[Introduction of new laboratory device 4SPIN® for nanotechnologies](#)

M. Pokorny, J. Rebíček, J. Klémes and V. Velebný	35
--	----

[Profile and material characterization of sine-like surface relief Ni gratings by spectroscopic ellipsometry](#)

J. Mistrik, R. Antos, M. Karlovec, K. Palka, Mir. Vlcek and Mil. Vlcek	36
--	----

[Preparation of sparse periodic plasmonic arrays by multiple-beam interference lithography](#)

M. Vala and J. Homola	37
-----------------------------	----

[High-performance biosensing on random arrays of gold nanoparticles](#)

B. Spackova, H. Sipova, N. S. Lynn, P. Lebruskova, M. Vala, J. Slaby and J. Homola	38
--	----

Nanofabrication by imprint lithography and its application to photonic devices

Y. Sugimoto,^{*} B. Choi, M. Iwanaga, N. Ikeda, H. T. Miyazaki, and K. Sakoda

National Institute for Materials Science (NIMS), 1-2-1 Sengen, Tsukuba, Ibaraki 305-0047, Japan

^{*}Electronic mail: sugimoto.yoshimasa@nims.go.jp

We fabricated a large area surface plasmon (SP) -RGB color filter consisting of periodic hole array in an aluminum (Al) film using ultra-violet (UV) nanoimprint lithography (NIL) and reactive ion etching. The diameter of the holes are 210 nm, 165 nm and 130 nm, and the lattice constants are 420 nm, 330 nm and 260 nm, for the red, green, and blue colors, respectively. Thus, a full color filter utilizing an SP in the Al film was successfully fabricated by NIL. We also fabricated large-area stacked complementary plasmonic crystals (SC PICs) by UV-NIL. The SC PICs were made on silicon-on-insulator (SOI) substrates consisting of three layers: the top layer contacting air was a perforated Au film, the bottom layer contacting the buried oxide layer included an Au disk array corresponding to the holes in the top layer, and the middle layer was a Si PC slab. The SC PICs have prominent resonances in optical wavelengths. We examined the photoluminescence (PL) enhancement of monolayer dye molecules on the SC PIC substrates in the visible range and found large PL enhancements of up to a 100-fold in comparison with dye molecules on nonprocessed Si wafers.

Nano-photonic structures/materials such as surface plasmon (SP) and meta material (MM) as well as photonic crystals (PCs) are discussed from potentials for new photonic devices and technologies. Plasmonics that deal with artificial metallic nanostructures is an emerging field to manipulate electromagnetic (EM) waves in the subwavelength dimensions [1, 2]. The fundamental aspect of light-matter interaction in locally enhanced EM fields is also attracting interest. Due to the development of fabrication technologies, numerous studies on plasmonics have been conducted, revealing many features of various plasmonic structures, such as nanospheres, nanorods, and nanoantenna. The optical transmission based on SP resonance (SPR) through periodic hole array in metallic film is attracting much attention. Because SP is expected to increase density of information by controlling and localizing of light beyond the diffraction limit, as well as saving energy through extraordinary optical transmission (EOT) [3]. It has been also reported that the plasmonic resonances mediate enhanced excitation and radiation processes; the resonant modes have even been effectively applied for controlling photoluminescence (PL) [4]. Still, it is a challenge to fabricate precisely controlled metallic nanostructures with areas greater than $10 \times 10 \text{ nm}^2$. Large-area plasmonic substrates are important in making functional plasmon-enhanced sensors [5]. Artificially controlled plasmonic nanostructures at the subwavelength scale are smaller than the available wavelength of illumination. The preparation of such subwavelength plasmonic nanostructures usually involves the use of expensive high-performance equipment for semiconductor mass production. Conventionally, direct-writing electron beam lithography (EBL) or focused ion-beam techniques are adopted for the fabrication of the nanoscale structures. However, these methods are slow and expensive, limiting their practical application for the fabrication of large-area surfaces. Given these considerations, NIL is considered to be an ideal solution for large-area patterning of nanoscale structures at relatively low cost [6, 7]. The NIL technique is based on the direct physical and mechanical deformation of the resist, making it suitable to obtain significantly high resolution, unlike conventional photolithography techniques associated with the light diffraction or scattering.

In this paper, we present the fabrication and transmission characteristics of a large-area, SP-*RGB* color filter consisting of a periodic hole array in an Al thin film fabricated by ultra-violet (UV)-NIL and reactive ion etching (RIE). We also demonstrate the fabrication, by UV-NIL technique, of large-scale, Au-coated, stacked complementary plasmonic crystals (SC-PICs) substrates composed of uniform nanohole arrays. The achieved surface structures strongly modify and enhance emission compared to the reference silicon wafer without SC-PICs [8].

When light passes through a hole in a metal, it can couple with guided modes or SP modes on the metal surface. For guided modes, the light energy is confined within the space between the edges, and wavelengths longer than the cut-off wavelength are not transmitted through the hole. For the case when the metal is a perfect conductor and the hole is a vacuum, this cut-off wavelength corresponds to half the hole width. In contrast, since SPs represent electron oscillations, and can pass along the inner wall under resonance conditions, light coupled to SPs can propagate through the hole, even if the

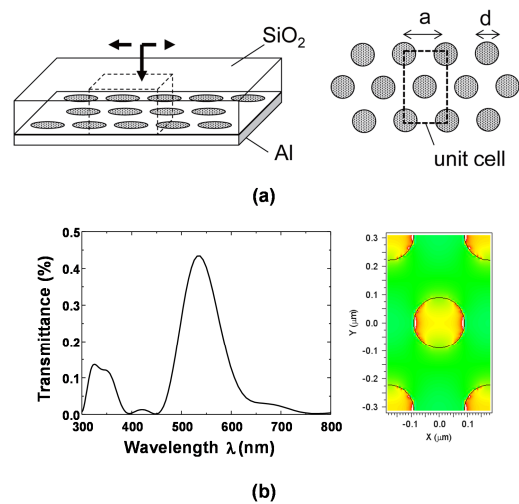


Figure 1. (a) Numerical calculation model of Al color filter with hole-array. (b) Calculated results of transmission spectrum and field distribution.

wavelength is longer than the cut-off wavelength [9, 10]. Based on this concept, the transmittance spectra for hole arrays in Al films were calculated using the finite difference time domain (FDTD) method. The model used for the calculation is shown in Fig. 1(a). For triangle lattice, lattice constant *a*, diameter of circle shape *d* and thickness of Al are set to 360nm, 180nm (= *a*/2) and 150nm, respectively. Al film was covered by a passivating SiO₂ layer (dielectric of index 1.5). Figure 1(b) shows the calculated transmittance spectra for hole diameter of 180 nm, which yield strong transmission in the green region. The electric field corresponding to a peak at $\lambda = 530 \text{ nm}$ in transmission spectrum shows a strong field distribution around hole. A normalized frequency, a/λ of resonance 0.64 correlated with the value calculated by theoretical analysis. Therefore, transmission occurs at wavelengths greater than twice the hole diameter.

Figures 2(a) and 2(b) show the measured transmission spectra of triangle lattices with circular and triangular holes, respectively. The insets show plan-view scanning electron microscopy (SEM) images of the circular and triangular holes, as well as transmission microscope images of the samples. For the circular holes, a peak transmittance of 44% and a FWHM of 130 nm were achieved when $a = 420 \text{ nm}$. For the triangular holes, a peak transmittance of 36% and a FWHM of 94 nm were achieved when $a = 420 \text{ nm}$. The spectra show shift of wavelength depending on lattice constant of hole array. A wavelength is equivalent to 1.5 times of the lattice constant (*a*) and is equivalent to 3 times of the diameter *d*. Also a peak wavelength λ for each lattice constant *a* shows good agreement to theoretical analysis and simulation result $a/\lambda = 0.64$. Since the incident illumination is white light, it is clear from this figure that effective color filtering can be achieved. Figure 2(c) shows a photograph of 3inch-size SP-*RGB* color

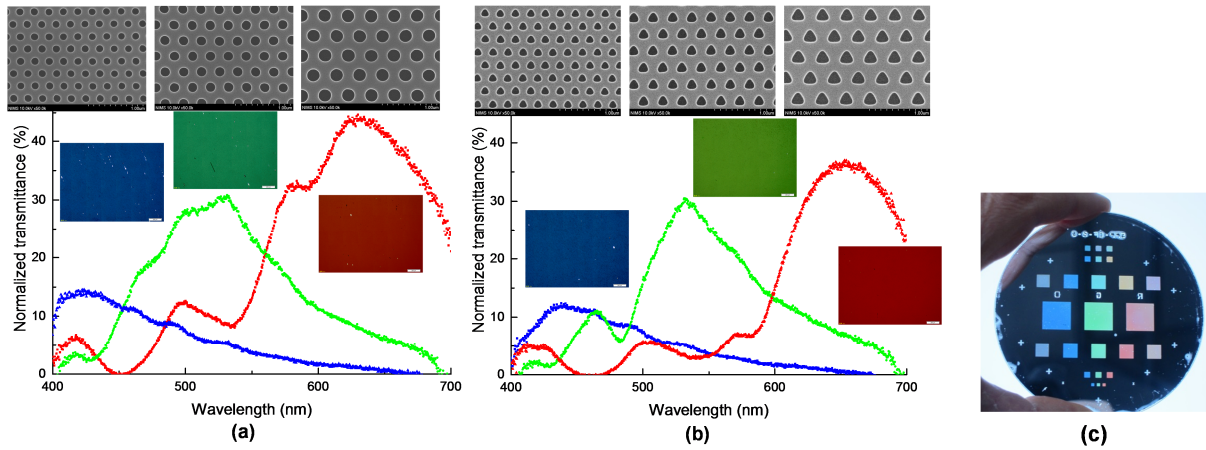


Figure 2. Transmission spectra of (a) triangle lattice of circle shape, (b) triangle lattice of triangle shape. Insets show the each optical microscope image and SEM image. (c) The photograph of a 3inch-size SP-RGB color filter.

filter based on a quartz substrate. This filter has triangular shaped holes, periodically arranged on an Al thin film (150 nm thick). The side of the triangles are 210 nm, 165 nm and 130 nm, and the lattice constants are 420 nm, 330 nm and 260 nm, for the red, green, and blue colors, respectively. Despite the fact that the side lengths are shorter than the wavelength of the visible light, the light has successfully penetrated the Al film. The maximum size of filter area is 10×10 mm square.

Figure 3(a) shows the schematic of an SC PIC substrate; the whole view (left) and section view (right) are drawn. The SC structure was conceived to make use of a feature suggested by Babinet's principle [11], which holds approximately true in actual systems including real metals with finite thickness. The principle implies that two structurally complementary layers have equi-wavelength hetero-resonances, so that when the two layers are closely located, the resonances in each layer couple and form new constructive resonances that are not simple bonding-anti-bonding states [12, 13]. The new resonances are featured in the SC structure. The SC PICs is composed of different sectional structures based on the silicon-on-insulator (SOI) wafer that contains three layers with two layers containing 2D triangular lattice of air holes, and one Au disks in the xy plane in the top SOI layer. The surface of top layer is covered with thin Au films. The middle layer is regarded as silicon photonic crystals slab with hole radius and lattice constant. In our scheme, the top and bottom layers are almost complementary to each other due to their constructive plasmonic coupling via middle hole layer. The two complementary layers have a 35 nm thick Au, and they are separated by the intermediate layer with a 200 nm thick of air hole. Comparing the calculated reflection

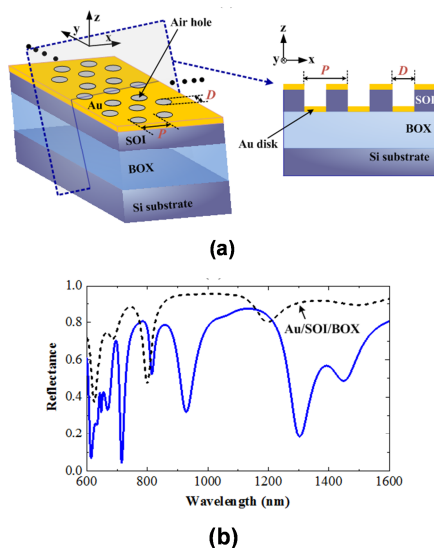


Figure 3. (a) Schematic illustrations of an SC PIC. Left: The whole view at an oblique angle. Right: Section view taken at the section indicated at the left. (b) The blue solid curve shows the calculated reflectance (R) spectrum for the SC PIC with periodicity $P = 410.5$ nm, hole diameter $D = 220$ nm, and SOI and BOX (SiO_2) layer thickness of 200 and 400 nm, respectively. The black dashed curve shows the calculated R spectrum of the Au/SOI/BOX multilayer structure without any hole.

efficiency, based on rigorous coupled-wave analysis, of the Au SC-PICs and an Au/SOI/BOX multilayer structure without any holes (Figure 3(b)), artificially engineered light manipulation can be achieved by employing Au SC-PICs.

Figure 4(a) shows the reflection spectra at normal incidence. The inset shows the imprinted resist pattern of the overall substrate. A 10×10 mm² imprinted area was clearly observed. The 24 spectra measured at different points of the Au SC-PIC substrate are plotted. The multiple spectra exhibit significant overlap. The averaged trough minimum corresponds to a reflection efficiency of 13.7% at a wavelength of 718 nm (position A). Therefore, the results at each of the 24 spots show an almost identical response compared with the results of other studies [14, 15]. The reflection spectra imply high spatial uniformity, which is enough to obtain the initially intended optical quality over the whole substrate surface. In addition, the measured result is in good agreement with the calculated reflection efficiency shown in Fig. 3(b). Distinct deep plasmonic resonances were observed at positions A and B, as obtained in the calculation. Because the calculations were implemented based on the ideal model of an Au SC PIC, the observed minor deviations in the reflection efficiency could come from the differences between the model and the actual fabricated structures. Figure 4(b) shows the measured PL enhancement in an SC PIC substrate with Rhodamine 6G (R6G). The enhancement factor is the ratio of the PL intensity observed from the dye molecules on an SC PIC substrate to that from molecules adsorbed on a reference substrate (or Si wafer). The inset shown in Fig. 4(b) shows the PL spectrum of the reference Si wafer with a pump power of 250 μW . The peak wavelength was about 610 nm. The PL spectrum from the Au SC PIC is strongly modified when compared with that of the reference substrate. The observed distinct peaks are attributed to the engineered plasmonic resonance effect, and the highest peak at 717 nm indicates a 100-fold increase in the PL intensity for SC PIC compared with the Si substrate. The large enhancement of the PL intensity on the SC PIC can be attributed to the nm indicates a 100-fold increase in the PL intensity for SC PIC compared with the Si substrate. The large enhancement of the PL intensity on the SC PIC can be attributed to the strong interaction

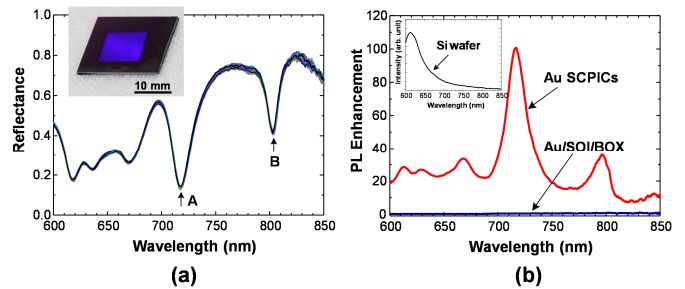


Figure 4. (a) Measured reflection spectra at normal incidence of the fabricated Au SC-PICs. The twenty-four spectra taken are overlaid. Inset shows the imprinted substrate with the two-dimensional hole array resist pattern. (b) Photoluminescence (PL) enhancement of the fabricated Au SC-PICs and Au/SOI/BOX structures on the same substrate. The inset shows the PL spectrum of R6G on the unprocessed Si wafer.

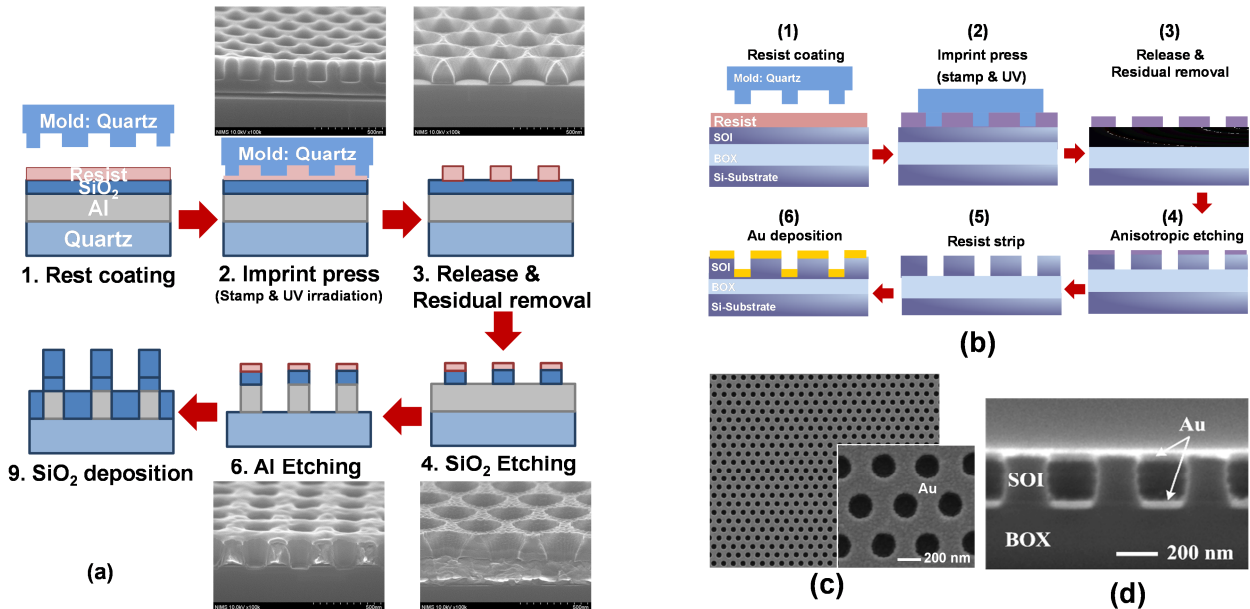


Figure 5. (a) Fabrication procedure of the SP-RGB color filter using the UV-NIL technique. Insets show SEM images for each process step. (b) Fabrication procedure for an Au SC-PIC using the UV-NIL technique. (c) Top-down view SEM images of fabricated Au SC-PICs. The SEM image shown in the inset reveals the uniformity of the holes and Au surface. (d) Section view SEM image of the Au SC-PICs with clearly indicated 35 nm thick Au layers at the top and bottom of the SOI layer.

between the excited dye molecules and plasmonic resonance modes. The wavelength of the strongly enhanced peaks corresponds to the measured reflection dips.

We have fabricated periodic hole arrays in Al films by UV-NIL and RIE. Transmission characteristic of devices were investigated in hole shape and lattice constant in the range of visible light. In a device with triangle lattice of circle hole, a transmittance of 44% and a FWHM of approximately 130nm are achieved. We have also successfully fabricated an emission-enhanced large-scale 2D Au SC-PICs by UV-NIL combined with RIE and metal deposition. The observed PL intensity of the fabricated structure with R6G was significantly increased by two-orders of magnitude compared with the PL intensity on a reference Si wafer. The fabricated structure showed intense troughs in the reflection spectra, with a measured value of about 14 % at 718 nm. It is assumed this behavior is caused by plasmonic resonance. A high uniformity was also confirmed by multiple reflection measurement which was included within ± 1 % variations at the dips. That means our nanoimprint fabrications can be applied to a high quality surface engineering substrate.

MATERIALS AND METHODS

The SP -RGB color filter fabrication procedure is presented in Fig. 5(a). Al of thickness 150nm was deposited on quartz substrate, and 50nm thick SiO₂ is deposited on Al. UV-NIL is used for patterning process of sub-micron periodic hole array. The used UV imprint equipment is ST-50 (Toshiba Machine Company). The resist of the pressed portion by the convex part of the mold disappears, and the transferred resist pattern is formed on the substrate. A pattern was transferred to SiO₂ layer by CHF₃-based RIE, were sequentially transferred to Al film by a Cl₂ based inductive coupling plasma RIE. After resist removal by O₂ plasma asher, device surface was covered with 50nm thick SiO₂ for index matching and prevention oxidation by plasma-enhanced chemical vapor deposition. Transmission spectra were measured by CCD multi-channel spectrometer and color images were observed by CCD camera at the same time using optical microscope system. A non-polarized halogen lamp was used as a light source.

The fabrication process for Au SC PICs is illustrated in Fig. 5(b). The used polymer resist is spin-coated on an SOI wafer (step 1). The prepared mold and substrate is set, then the mold is pressed against the substrate under the programmed sequential process for the irradiation power and time control (step 2). The imprinted substrate is followed by a short etching step to remove the residual or scum (step 3). For the imprinted pattern transfer to the SOI layer, the anisotropic plasma RIE is carried out using a Bosch process with SF₆ and C₄F₈ gas for the alternated cycles of etching and passivation, respectively (step 4). After removal of resist layer, finally, a 35-nm-thick Au film is deposited (step 5-6). Optical characterization of the fabricated SC PICs is performed from the Au surface of the substrate. The finally fabricated Au SC-PICs structure is presented in Fig. 5 (c). The obtained hole diameter was 215 nm which is almost same with the size of master mold design. The cross section of completed Au SC PICs is shown in Fig. 5 (d). A 35-nm-thick Au layer is clearly observed in the top and bottom layers. Consequently, any distinguished Au particles are not noticeable at the SOI walls. In order to explore the emission enhancement, we studied dye molecules of Rhodamine 6G (R6G) on the fabricated Au SC PICs structure. The starting solutions of R6G in methanol had a concentration of 1×10^{-5} M, and followed by the coating of solutions on the surface of imprinted

sample and non-processed silicon wafer for comparison. For the evaluation of resonant reflection and emission spectra of Au SC PICs with R6G at room temperature, we have constructed a micro-spectroscopy system composed of an objective, achromatic imaging lenses, and a CCD camera for normal direction measurement. Reflection spectra of the arrayed SC-PICs were obtained by a cooled CCD detector array through a multimode fiber and a spectrometer. Polarized, collimated white light from a tungsten halogen lamp was used for the reflection spectra. Emission spectra measurement was carried out by using the same spectroscopy system for the pump by a continuous-wave diode pumped solid state laser with a wavelength of 532 nm. The collimated pump laser via Neutral Density (ND) filter was focused to a 25- μ m-diameter spot on the sample surface.

ACKNOWLEDGEMENT

This study was supported by a Grant-in-Aid for Scientific Research on Innovative Areas from the Japanese Ministry of Education, Culture, Sports and Technology (Grant number 22109007). Also, a part of this work was supported by Nano-Integration Foundry, Low Carbon Research Network in National Institute for Materials Science (NIMS), Japan.

REFERENCES

- [1] E. Ozbay, Plasmonics: merging photonics and electronics at nanoscale dimensions, *Science* **311**, 189–193 (2006).
- [2] J. A. Schuller, E. S. Barnard, W. Cai, Y. C. Jun, J. S. White, M. L. Brongersma, Plasmonics for extreme light concentration and manipulation, *Nat. Mater.* **9**, 193–204 (2010).
- [3] T. W. Ebbesen, H. J. Lezec, H. F. Ghaemi, T. Thio, P. A. Wolff, Extraordinary optical transmission through sub-wavelength hole arrays, *Nature* **391**, 667–669 (1998).
- [4] A. M. Glass, P. F. Liao, J. G. Bergman, D. H. Olson, Interaction of metal particles with adsorbed dye molecules: absorption and luminescence, *Opt. Lett.* **5**, 368–370 (1980).
- [5] K. A. Willets, R. P. Van Duyne, Localized surface plasmon resonance spectroscopy and sensing, *Annu. Rev. Phys. Chem.* **58**, 267–297 (2007).
- [6] S. Y. Chou, P. R. Krauss, P. J. Renstrom, Imprint of sub-25 nm vias trenches in polymer, *Appl. Phys. Lett.* **67**, 3114–3116 (1995).
- [7] L. J. Guo, Nanoimprint lithography: Methods and materials requirements, *Adv. Mater.* **19**, 495–513 (2007).
- [8] B. Choi, M. Iwanaga, H. T. Miyazaki, K. Sakoda, Y. Sugimoto, Photoluminescence-enhanced plasmonic substrates fabricated by nanoimprint lithography, *J. Micro/Nanolith. MEMS MOEMS* **13**, 023007 (2014).
- [9] D. Inoue, T. Nomura, A. Miura, H. Fujikawa, K. Sato, N. Ikeda, D. Tsuya, Y. Sugimoto, Y. Koide, K. Asakawa, Polarization independent RGB color filter comprising an aluminum film with surface plasmon enhanced transmission through a sub-wavelength array of holes, *Appl. Phys. Lett.* **98**, 093113 (2011).
- [10] D. Inoue, T. Nomura, A. Miura, H. Fujikawa, K. Sato, N. Ikeda, D. Tsuya, Y. Sugimoto, Y. Koide, Polarization filters for visible light consisting of sub-wavelength slits in an aluminum film, *J. of Lightwave Technology* **30**, 3463–3467 (2012).
- [11] F. J. García de Abajo, Light scattering by particle and hole arrays, *Rev. Mod. Phys.* **79**, 1267–1290 (2007).

- [12] M. Iwanaga, Subwavelength electromagnetic dynamics in stacked complementary plasmonic crystal slabs, *Opt. Express* **18**, 15389–15398 (2010).
- [13] M. Iwanaga, Electromagnetic eigenmodes in a stacked complementary plasmonic crystal slab, *Phys. Rev. B* **82**, 155402 (2010).
- [14] D. Chanda, K. Shigeta, S. Gupta, T. Cain, A. Carlson, A. Mihi, A. J. Baca, G. R. Bogart, P. Braun, J. A. Rogers, Large-area flexible 3D optical negative index metamaterial formed by nanotransfer printing, *Nat. Nanotechnol.* **6**, 402–407 (2011).
- [15] J. Yao, A.-P. Le, S. K. Gray, J. S. Moore, J. A. Rogers, R. G. Nuzzo, Functional nanostructured plasmonic materials, *Adv. Mater.* **22**, 1102–1110 (2010).